

Supplementary Information for

**Gold film deposition by infrared laser photothermal treatment on 3D-printed electrodes: electrochemical performance enhancement and application**

*William B. Veloso<sup>1</sup>, Gabriel N. Meloni<sup>1</sup>, Iana V. S. Arantes<sup>1</sup>, Lauro A. Pradela-Filho<sup>1</sup>, Rodrigo A. A. Muñoz<sup>2</sup> and Thiago R. L. C. Paixão<sup>1</sup>.*

<sup>1</sup> Institute of Chemistry, Department of Fundamental Chemistry, University of São Paulo, 05508-000, São Paulo, SP, Brazil.

<sup>2</sup> Institute of Chemistry, Federal University of Uberlândia, 38400-902, Uberlândia, MG, Brazil.

**Summary**

1. Printing parameters and assembly of 3D-printed electrodes.....	2
2. Optimization of IR-laser parameters for 3D-CB/PLA electrodes surface pre-treatment.....	3
3. Optimisation of modification parameters.....	4
3.1. IR-laser parameters .....	4
3.2. Drop-casting parameters .....	6
4. EDS analysis .....	8
5. Voltammogram of 3D-printed electrodes in supporting electrolyte .....	8
6. Electrochemical impedance spectroscopy.....	9
References .....	10

## 1. Printing parameters and assembly of 3D-printed electrodes

The polymeric electrode parts were printed employing two different 3D printing technologies (FDM and MSLA). A cylindrical CB/PLA substrate (Fig S1A), used as the electrodic surface, was printed using an FDM 3D printer (Adventurer 4, FlashForge, China) loaded with a commercial conductive filament CB/PLA-based. The main printing parameters used in this stage were: nozzle temperature of 210 °C, bed temperature of 60 °C, printing speed of 50 mm s<sup>-1</sup>, layer height of 0.1 mm, and infill percentage of 100%. The electrode housing was printed in two pieces to facilitate the assembly process, using an MSLA 3D printer (Elegoo, China) loaded with a light-curing ABS-like resin. The main parameters for electrode housing printing were: layer height of 0.05 mm, bottom layer exposure of 20 s, normal exposure of 2.5 s, bottom layer retraction speed of 60 mm s<sup>-1</sup>, and normal retraction speed of 110 mm s<sup>-1</sup>. After printing, the electrodes were assembled by fixing the lower and upper part of the electrode housing using the same resin used for printing and exposing it to a source of UV radiation for 20 minutes. Subsequently, the electrodes were sanded using 600-grit sandpaper until a smooth surface was obtained (Fig. S1B).

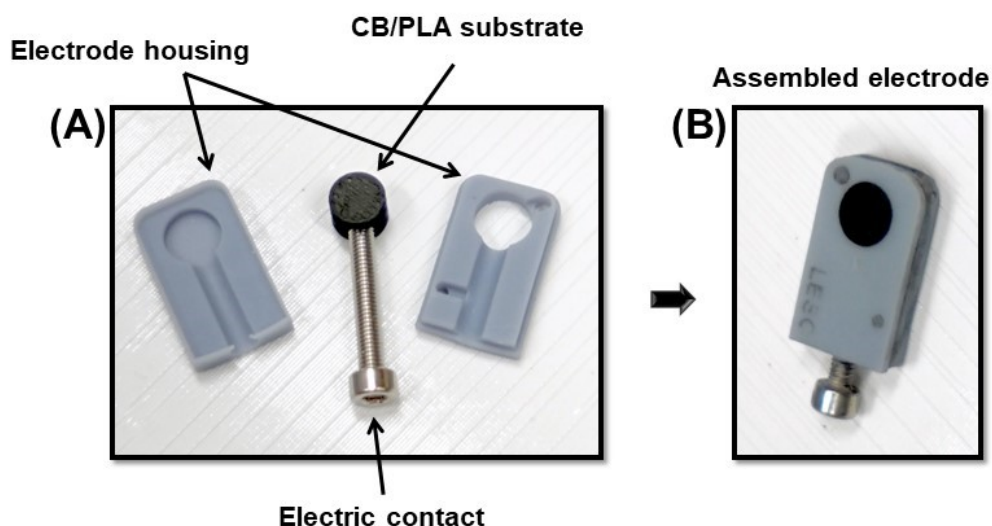


**Fig S1:** (A) Image of the parts that comprise the 3D-printed electrodes. (B) Assembled 3D-printed electrode.

## 2. Optimization of IR-laser parameters for 3D-CB/PLA electrodes surface pre-treatment

Each adjustable parameter of the IR-laser used for pre-treating the 3D-printed electrodes was assessed individually by measuring the surface electrical resistance. The measurements were carried out using a digital multimeter. The multimeter's probes were placed over the treated area at a constant distance of 5 mm, and the test probe was held on the surface with a constant, and similar among all measurements, pressure, as illustrated in Fig. S2. Although the amount of pressure is somewhat abstract and resistance values are only semi-qualitative when acquired in this procedure, if it is kept constant between measurements, it provides enough precision to compare parameters, as highlighted by the small error bars in Fig. 2 of the main manuscript. The influence of power was verified, keeping the beam scan rate and focal distance constant. Next, the power and scan rate were kept constant, and the focal distance was varied. Finally, the laser power and focal distance were kept constant, and the beam scan rate was changed. Each parameter chosen was used in the subsequent optimisation, and each measurement was performed in triplicate ( $n = 3$ ).

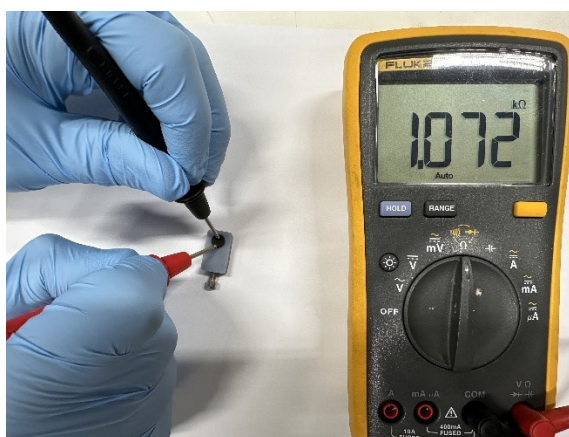


Fig. S2 – Photo of the resistance being measured.

### 3. Optimisation of modification parameters

The modification parameters were optimised based on the voltammetric response in the presence of  $5.0 \text{ mmol L}^{-1} [\text{Fe}(\text{CN})_6]^{3-/4-}$ . The IR-laser parameters for gold reduction and drop-casting conditions were selected based on the reversibility criteria of the voltammograms obtained in the presence of the redox probe. This included a peak-to-peak separation closer to  $57 \text{ mV}/n$  (in this case,  $n = 1$ ) and a ratio of the anodic peak to the cathodic peak closer to one.<sup>1</sup> The ideal value was chosen based on these reversibility criteria with a lower standard deviation ( $n = 3$ ).

#### 3.1. IR-laser parameters

Initially, the power of the IR-laser was optimised in the range of 0.3 to 1.0 W. This range was established based on the level of damage to the substrate. Laser power of up to 0.3 W was insufficient to cause any changes to the material surface, whereas laser power beyond 1.0 W destroyed the substrate. These powers correspond to the real power emitted by the equipment. These values were measured by placing a power meter (Synrad PW-250) between the gantry and the head mirrors. Fig. S3 displays the voltammograms and the relationship between  $I_p$  and  $\Delta E_p$  with laser power.

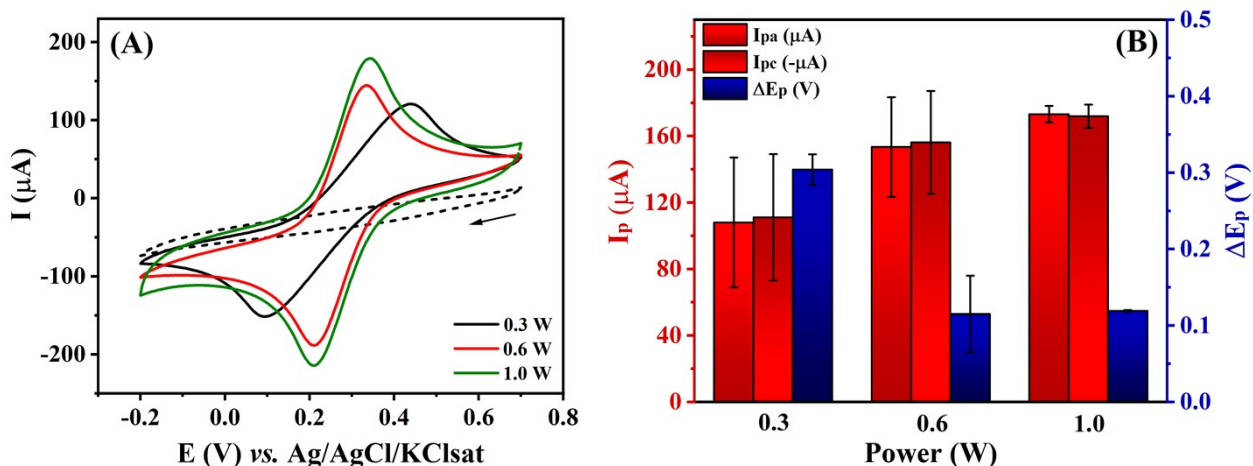


**Fig. S3** – (A) CVs recorded using modified 3D-CB/PLA electrodes obtained at different IR-laser powers (0.3 – 1.0 W) in the absence (dashed trace) and presence (solid trace) of  $5.0 \text{ mmol L}^{-1} [\text{Fe}(\text{CN})_6]^{3-/4-}$  in  $1.0 \text{ mol L}^{-1} \text{ KCl}$  as supporting electrolyte; scan rate of  $20 \text{ mV s}^{-1}$ . (B) Relationship between  $I_{pa}$ ,  $I_{pc}$  and  $\Delta E_p$  with laser power.

The impact of laser distance on electrode modification was studied by placing the substrate at various focal distances ranging from 7.0 to 13.0 mm using a laser power of 1 W. The distance range was determined based on the distance limits set for the equipment. The tests were conducted in the same manner as described earlier, and the outcomes are illustrated in Fig. S4.

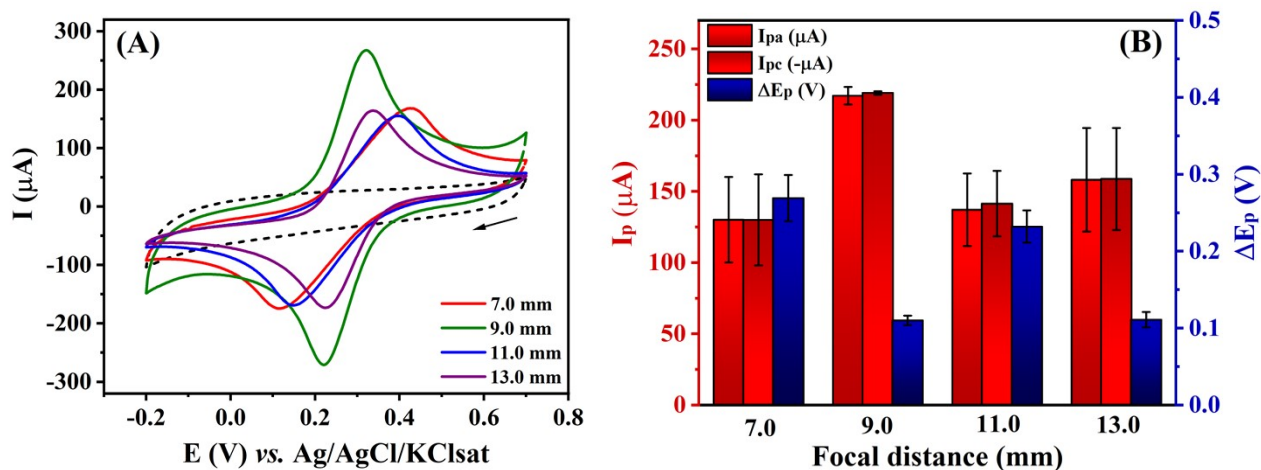


**Fig. S4** – (A) CVs recorded using modified 3D-CB/PLA electrodes obtained at different focal distances (7.0 – 13.0 mm) in the absence (dashed trace) and presence (solid trace) of  $5.0 \text{ mmol L}^{-1} [\text{Fe}(\text{CN})_6]^{3-/4-}$  in  $1.0 \text{ mol L}^{-1} \text{ KCl}$  as supporting electrolyte; scan rate of  $20 \text{ mV s}^{-1}$ . (B) Relationship between  $I_{pa}$ ,  $I_{pc}$  and  $\Delta E_p$  with laser focal distance.

The effect of beam scan rate was investigated in a range of 1.0 to 10 mm s<sup>-1</sup> using a laser power of 1.0 W and a focal distance of 9.0 mm. The tests were conducted in the presence of 5.0 mmol L<sup>-1</sup> [Fe(CN)<sub>6</sub>]<sup>3-/4-</sup>, and the results are illustrated in Fig. S5.

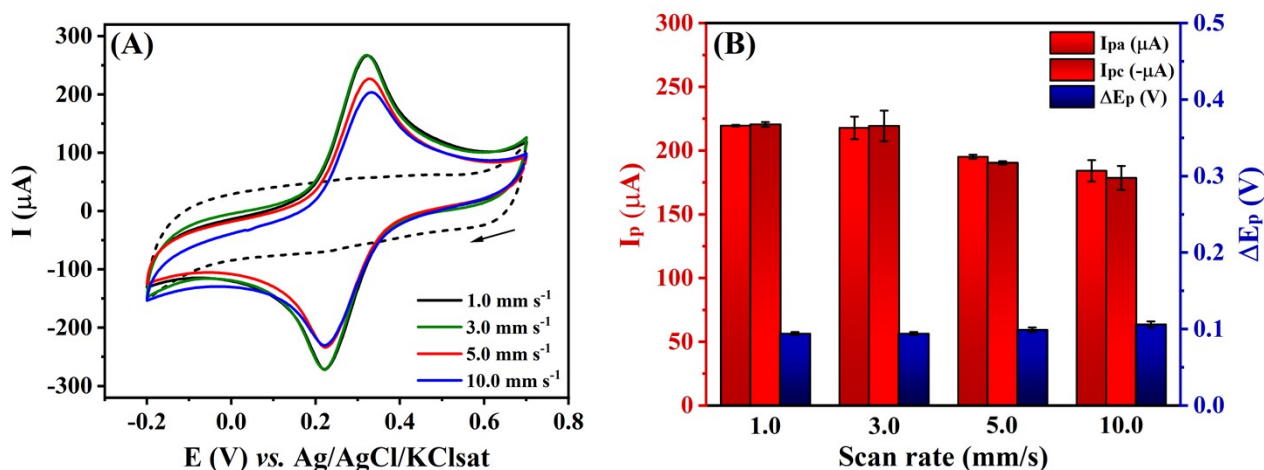
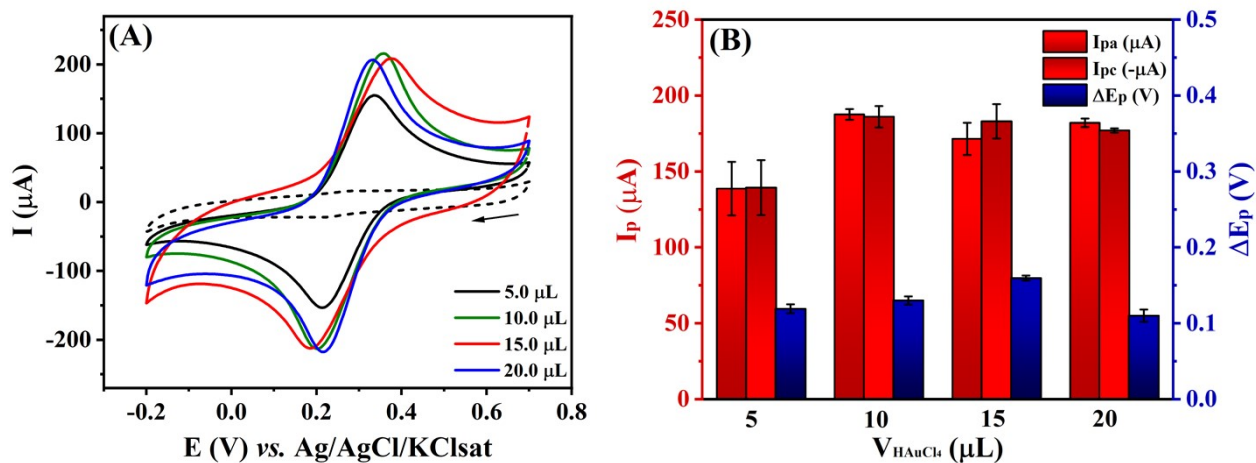


Fig. S5 – (A) CVs recorded using modified 3D-CB/PLA electrodes obtained at different laser scan rates (1.0 – 10.0 mm s<sup>-1</sup>) in the absence (dashed trace) and presence (solid trace) of 5.0 mmol L<sup>-1</sup> [Fe(CN)<sub>6</sub>]<sup>3-/4-</sup> in 1.0 mol L<sup>-1</sup> KCl as supporting electrolyte; scan rate of 20 mV s<sup>-1</sup>. (B) Relationship between  $I_{pa}$ ,  $I_{pc}$  and  $\Delta E_p$  with laser scan rate.

### 3.2. Drop-casting parameters

The volume and concentration of the H<sub>2</sub>AuCl<sub>4</sub> solution, used as the gold source at the drop-casting step, were evaluated to obtain a gold film with the best possible electrochemical performance. Initially, the volume of solution was studied in an interval from 5  $\mu\text{L}$  to 20  $\mu\text{L}$  using a 30 mmol L<sup>-1</sup> H<sub>2</sub>AuCl<sub>4</sub> solution. Fig. S6 shows the results obtained in the volume study. The concentration of H<sub>2</sub>AuCl<sub>4</sub> was also investigated in the range of 5 - 40 mmol L<sup>-1</sup>, and the findings are displayed in Fig. S7.



**Fig. S6** – (A) CVs recorded using modified 3D-CB/PLA electrodes obtained at different  $30 \text{ mmol L}^{-1}$   $\text{HAuCl}_4$  solution volumes (5.0 – 20.0  $\mu\text{L}$ ) in the absence (dashed trace) and presence (solid trace) of  $5.0 \text{ mmol L}^{-1}$   $[\text{Fe}(\text{CN})_6]^{3-/4-}$  in  $1.0 \text{ mol L}^{-1}$  KCl as supporting electrolyte; scan rate of  $20 \text{ mV s}^{-1}$ . (B) Relationship between  $I_{pa}$ ,  $I_{pc}$  and  $\Delta E_p$  with  $\text{HAuCl}_4$  solution volume.

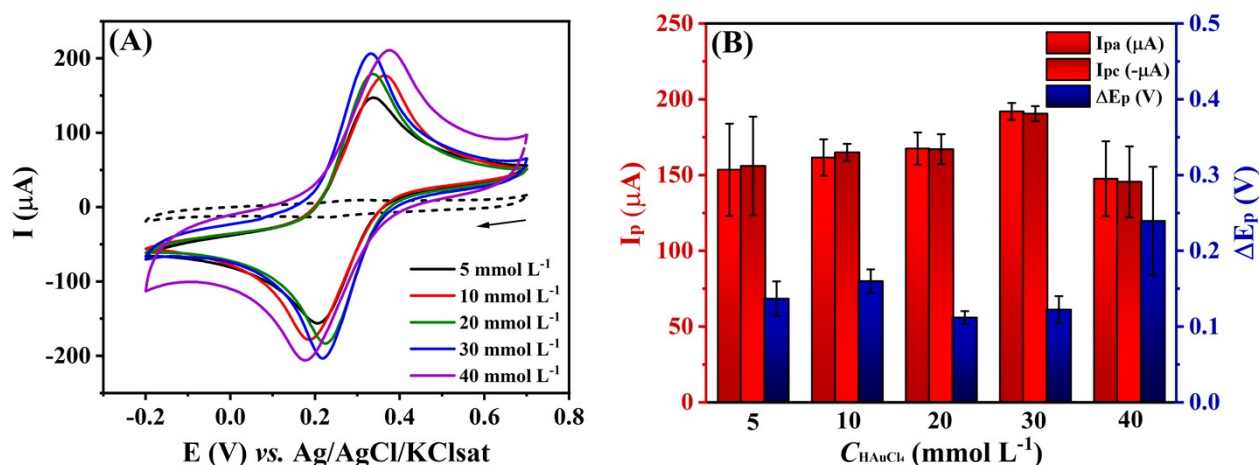


**Fig. S7** – (A) CVs recorded using modified 3D-CB/PLA electrodes obtained at different  $\text{HAuCl}_4$  solution concentrations (5.0 – 40.0  $\text{mmol L}^{-1}$ ) in the absence (dashed trace) and presence (solid trace) of  $5.0 \text{ mmol L}^{-1}$   $[\text{Fe}(\text{CN})_6]^{3-/4-}$  in  $1.0 \text{ mol L}^{-1}$  KCl as supporting electrolyte; scan rate of  $20 \text{ mV s}^{-1}$ . (B) Relationship between  $I_{pa}$ ,  $I_{pc}$  and  $\Delta E_p$  with  $\text{HAuCl}_4$  solution concentration.

#### 4. EDS analysis

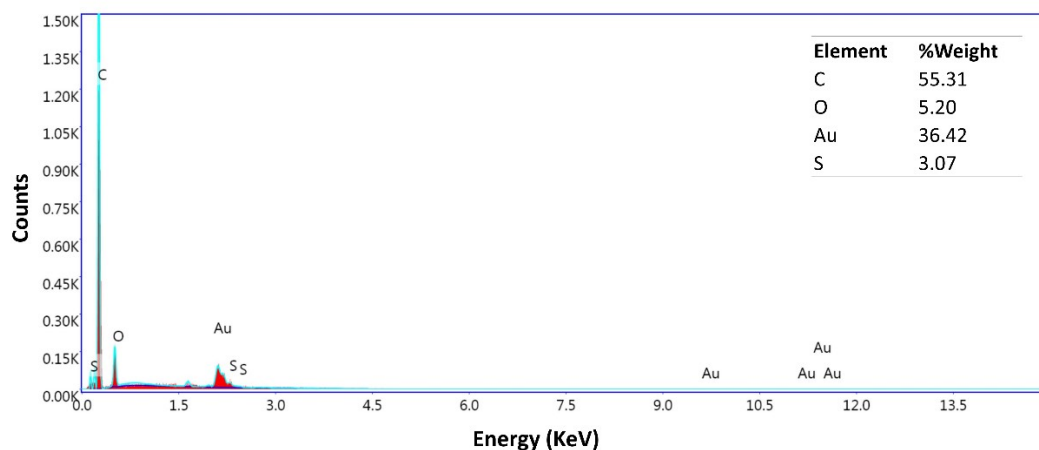


Fig. S8 - EDS spectra for modified 3D-CB/PLA.

Besides carbon, oxygen and gold, the EDS spectrum showed the presence of a small amount of sulphur in the sample. This element may come from impurities from the filament itself, as previously reported,<sup>2</sup> as well as from the  $H_2SO_4$  solution used for modifier preparation.

#### 5. Voltammogram of 3D-printed electrodes in supporting electrolyte

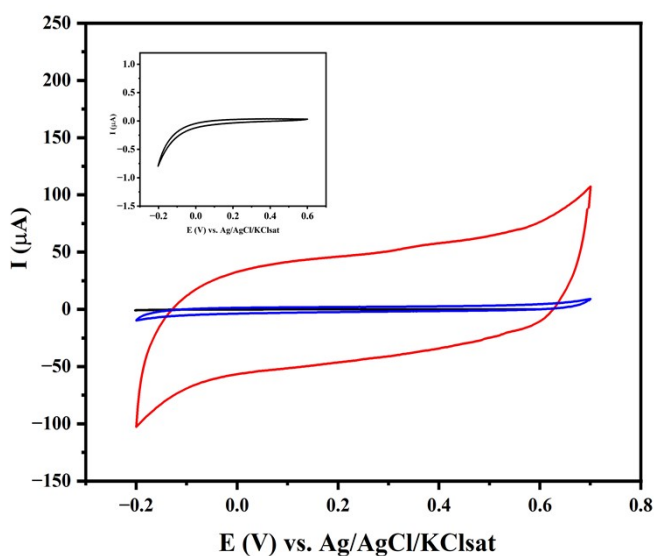
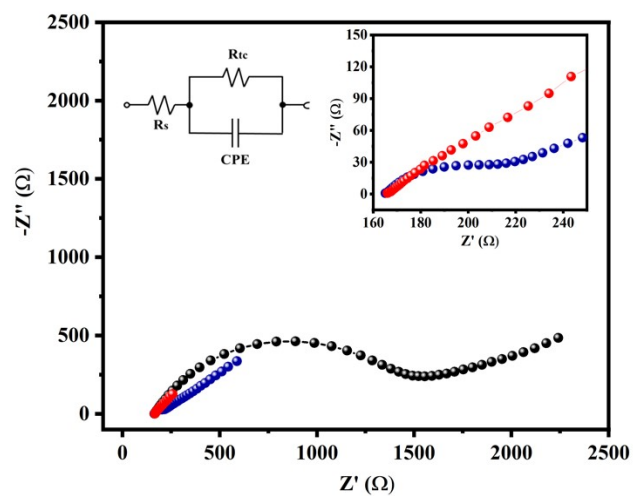


Fig. S9 – Cyclic voltammograms of 3D-CB/PLA (black trace), treated 3D-CB/PLA (blue trace) and modified 3D-CB/PLA (red trace) recorded in  $1.0 \text{ mol L}^{-1} \text{ KCl}$  at  $20 \text{ mV s}^{-1}$ . Insert: highlight for the voltammogram of 3D-CB/PLA electrode.



## 6. Electrochemical impedance spectroscopy



**Fig. S10** – Nyquist plots obtained from EIS using 3D-CB/PLA (black), treated 3D-CB/PLA (blue), and modified 3D-CB/PLA (red) in  $1.0 \text{ mol L}^{-1}$  KCl containing  $5.0 \text{ mmol L}^{-1}$   $[\text{Fe}(\text{CN})_6]^{3-/4-}$  over the frequency range from 100 kHz to 0.1 Hz with a modulation amplitude of 10 mV. The equivalent circuit is inserted in the graphic.

## References

- 1 A. J. Bard and L. R. Faulkner, *Electrochemical Methods: fundamentals and applications*, John Wiley & Sons, New York, Second., 2001.
- 2 E. M. Richter, D. P. Rocha, R. M. Cardoso, E. M. Keefe, C. W. Foster, R. A. A. Munoz and C. E. Banks, *Anal. Chem.*, 2019, **91**, 12844–12851.